**2017 IEEE/RSJ International Conference on Intelligent Robots and Systems (IROS)**
**September 24–28, 2017, Vancouver, BC, Canada**

# A Distributed Control Framework for a Team of Unmanned Aerial Vehicles for Dynamic Wildfire Tracking

Huy X. Pham, Hung M. La, *Senior Member, IEEE,* David Feil-Seifer, and Matthew Deans

***Abstract*— Wild-land fire fighting is a hazardous job. A key task for firefighters is to observe the "fire front" to chart the progress of the fire and areas it will likely spread next. Lack of information of the fire front causes many accidents. Using Unmanned Aerial Vehicles (UAV) to cover wildfire is promising because it can replace humans for fire tracking, reducing hazards and saving operation costs. In this paper we propose a distributed control framework designed for a team of UAVs that can closely monitor a wildfire in open space, and precisely track its development. The UAV team, designed for flexible deployment, can effectively avoid in-flight collisions and cooperate well with neighbors. They can maintain a certain height level to the ground for safe flight above fire. Experimental results are conducted to demonstrate the capabilities of the UAV team in covering a spreading wildfire.**

## I. Introduction

Wildfire is well-known for their destructive ability to inflict massive damages and disruptions. According to the U.S. Wildland Fire, an average of 70000 wildfires annually burn around 7 million acres of land and destroy more than 2600 structures [1]. Wildfire fighting is dangerous and time sensitive; lack of information about the current state and the dynamic evolution of fire contributes to many accidents [2]. Firefighters may easily lose their life if the fire unexpectedly propagates over them (Figure 1). Therefore, it is important to precisely cover the development of the fire and track its spreading boundaries. The more information regarding the fire spreading areas collected, the more effectively a scene commander could formulate a plan to evacuate people and properties out of danger zones, and prevent a fire from spreading to new areas.

Unmanned Aerial Vehicles (UAV) can be used to assist in wildfire fire tracking tasks and replace the use of manned helicopters, saving sizable operation costs [3], [4]. Accurate UAV-based fire detection has been effectively developed using means such as infrared cameras [3], analyzing fire segmentation in different color spaces [5], or using color indices to distinguish fire from smoke and steam [4]. Cameras play a crucial role in capturing the raw information for higher level detection algorithms. Specific applications in wildfire monitoring involving multiple robots systems have

Fig. 1. A wildfire outbreaks in California. Firefighting is really dangerous without continuous fire fronts growth information. Courtesy of USA Today.

been reported. Multiple UAVs can be commanded to track a spreading fire using checkpoints calculated based on visual images of the fire perimeter [6]. Artificial potential field have been used to control a team of UAVs in two separated tasks: tracking the boundary of a wildfire and suppressing it [7]. A centralized optimal task allocation problem is formulated in [8] to generate a set of waypoints for UAVs for shortest path planning.

Research that discusses the application of UAVs in assisting fire fighting remains limited, however [9]. To the best of the authors' knowledge, the above mentioned work does not cover the behaviors of their system when the fire is spreading. Works in [6] and [8] centralized the decision making, thus potentially overloading computation and communication when the fire in large scale demands more UAVs. The team of UAVs in [7] can continuously track the boundary of the spreading fire but largely depends on the accuracy of the modeled shape function of the fire in control design.

In this paper, we propose a decentralized control algorithm for a team of UAVs that can autonomously and actively track the fire spreading boundaries in a distributed manner, without dependency on the wildfire modeling. The UAVs can effectively share the vision of the field, while maintaining safe distance in order to avoid in-flight collision. Moreover, during tracking, the proposed algorithm can allow the UAVs to increase image resolution captured on the border of the wildfire. This idea is greatly inspired by the work of Schwager et al. in [10], where a decentralized control strategy was developed for a team of robotic cameras to minimize the information loss over an environment. For safety reasons, the UAV can also maintain a certain height level to the ground to avoid getting caught by the fire.

The rest of the paper is organized as follows: Section 2 discusses how wildfire spreading can be modeled as an objective for this paper. In Section 3, the wildfire tracking problem is formulated with clear objectives. In Section 4,

Huy Pham is a PhD student, and Dr. Hung La is the director of the Advanced Robotics and Automation (ARA) Laboratory. Dr. David Feil-Seifer is an Assistant Professor at Department of Computer Science and Engineering, University of Nevada, Reno, NV 89557, USA. Dr. Matthew Deans is with NASA Ames Research Center, Moffett Field, CA 94035.

This material is based upon work supported by the National Aeronautics and Space Administration (NASA) Grant No. NNX15AI02H issued through the Nevada NASA Research Infrastructure Development Seed Grant, and the National Science Foundation Cyber-Human Systems (NSF-CHS) Grant No. IIS-152 8137. Corresponding author: Hung La, email: hla@unr.edu

we propose a control design capable of solving the problem. A simulation scenario on Matlab are provided in Section 5. Finally, we draw a conclusion, and suggest directions for future work.

## II. Wildfire Modeling

Wildfire spreading simulation has attracted significant research efforts over the past decades, due to the potential in predicting wildfire spreading. Rothermel in 1972 [11] developed basic fire spread equations to mathematically and empirically calculate rate of speed and intensity. Richards [12] introduced a technique to estimate fire fronts growth using an elliptical model. These previous research were later developed further by Finney [13] and became a well-known fire growth model called Fire Area Simulator (FARSITE). Among existing systems, FARSITE is the most reliable model [14], and widely used by federal land management agencies such as U.S. Department of Agriculture Forest Service. However, in order to implement the model precisely, we need significant information regarding geography, topography, conditions of terrain, fuels, and weather. Since pursuing an accurate fire growth model is not our focus in this paper, we simplified the fire spreading propagation in FARSITE model to describe the fire fronts growth as follows:

$$\begin{aligned} X_t &= c \sin \Theta \\ Y_t &= c \cos \Theta. \end{aligned} \tag{1}$$

where $X_t$ and $Y_t$ are the differentials of the fire a long $x$ and $y$-axis in the plain, $\Theta$ is the azimuth angle of the wind direction and y-axis ($0 \leq \Theta \leq 2\pi$). $\Theta$ increases following clock-wise direction. $c$ is the distance from the fire source (ignition point) to the center of the ellipse. We can empirically calculate $c$ as follows [13]:

$$\begin{aligned} c &= \frac{R - \frac{R}{HB}}{2} \\ HB &= \frac{LB + (LB^2 - 1)^{0.5}}{LB - (LB^2 - 1)^{0.5}} \\ LB &= 0.936e^{0.2566U} + 0.461e^{-0.1548U} - 0.397, \end{aligned} \tag{2}$$

where $R$ is the steady-state rate of fire spreading. $U$ is the scalar value of mid-flame wind speed, calculated from actual wind speed value after taking account of the wind resistance by the forest. The new fire front location after time step $\Delta t$ is calculated as:

$$\begin{aligned} x_f(t + \Delta t) &= x_f(t) + X_t(t)\Delta t \\ y_f(t + \Delta t) &= y_f(t) + Y_t(t)\Delta t. \end{aligned} \tag{3}$$

Additionally, in order to simulate the intensity caused by fire around each fire front source, we also assume that each fire front source would radiate energy to the surrounding environment resembling a multivariate normal distribution probability density function of its coordinates $x$ and $y$. Assuming the intensity of each point in the field is a linear summation of intensity functions caused by multiple fire front sources, we have the following equation describing the intensity of each point in the wildfire caused by a number of $k$ sources:

$$I(x, y) = \sum_{i=1}^{k} \frac{1}{2\pi\sigma_{x_i}\sigma_{y_i}} e^{-\frac{1}{2}[\frac{(x-x_f)^2}{\sigma_{x_i}^2} + \frac{(y-y_f)^2}{\sigma_{y_i}^2}]}, \tag{4}$$

where $I(x, y)$ is the intensity of the fire at a certain point $q(x, y)$, $(x_f, y_f)$ is the location of the heat source $i$, and $(\sigma_{x_i}, \sigma_{y_i})$ are deviations. The point closer to the heat source has a higher level of intensity of the fire. A simulated wildfire spreading was represented in Figure 4.

## III. Problem formulation

Our objective is to control a team of multiple UAVs for collaboratively covering a wildfire and tracking the fire front propagation. We define covering to mean the UAVs are able to take multiple sub-pictures of the affected area so that most of the field is captured. We assume each UAV is equipped with localization devices (such as GPS and IMU), and identical downward-facing cameras capable of detecting fire. Each camera has a rectangular *field of view* (FOV). When covering, the camera and its FOV form a pyramid with half-angles $\theta^T = [\theta_1, \theta_2]^T$ (see Figure 2). Each UAV will capture the area under its FOV using its camera, and record the information into a number of pixels. We also assume that a UAV can maintain communication and exchange information with all other UAVs during the entire mission. Let $N$ denote the set of the UAVs. Let $p_i = [c_i^T, z_i]^T$denote the pose of a UAV $i \in N$. In which, $c_i^T = [x_i, y_i]^T$ indicates the lateral coordination, and $z_i$ indicates the altitude. Let $B_i$ denote the area that lie inside the field of view of UAV $i$, while $l_{k,i}, k = 1 : 4$ denotes each edge of the rectangular FOV of UAV $i$. The team of UAV needs to satisfy the following objectives to reach our goals.

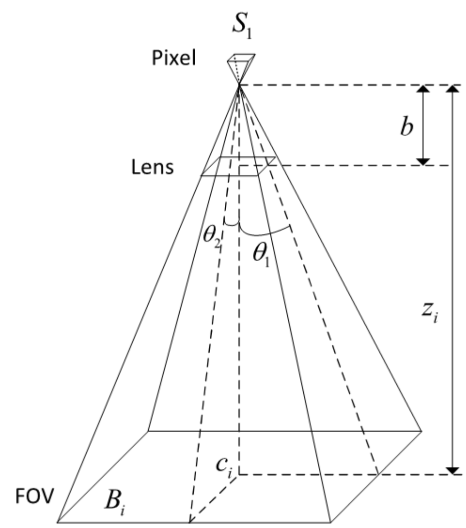


Fig. 2. Rectangular field of view of a UAV, with half-angles $\theta_1$, $\theta_2$. Each UAV will capture the area under its field of view using its camera, and record the information into a number of pixels.

### A. Deployment objective

The UAVs can be deployed from depots distributed around the forest, or from a forest firefighting department center.

When a wildfire occurs, its initial location is reported to a team of UAVs. Upon receiving the report of a wildfire happening, the UAVs are commanded to start and move to the point where the location of the fire was initially observed. We call this point a rendezvous point $p_r = [p_x, p_y, p_z]^T$. The UAVs would keep moving toward this point until they can detect the wildfire inside their FOV.

### B. Collision avoidance and safety objective

The team of UAVs must be able to avoid in-flight collision. For UAV $i$ to avoid other neighbor UAV $j$, they must keep their distance not less than a designed distance $d$:

$$||p_j - p_i|| \geq d. \tag{5}$$

As we proposed earlier, during the implementation of the tracking and coverage task, the UAVs can lower their altitude to increase the resolution of the border of the wildfire. Since there is no obvious guarantee about the minimum altitude of a UAV, they can keep lowering their altitude, and may catch fire during their mission. Therefore, it is imperative that the UAVs must maintain a safe distance to the ground. We also use a similar repulsive force as in (21), but this time to push the UAV away from its image on the environment plane. Suppose the safe altitude is $z_{min}$, and infer the position of the image of the UAV $i$ as $p_{i'} = [c_i^T, 0]$, we have the safe altitude condition:

$$||p_i - p_{i'}|| \geq z_{min}. \tag{6}$$

### C. Coverage and tracking objective

Let $Q(t)$ denote the wildfire varying over time $t$ on a plane. The general optimal coverage problem is normally represented by a coverage objective function [15]–[18] with the following form:

$$\min H(p_1, ..., p_n) = \int_{Q(t)} f(q, p_1, p_2, ..., p_n)\phi(q, t)dq, \tag{7}$$

where $f(q, p_1, p_2, ..., p_n)$ represents some cost to cover a certain point $q$ of the environment. The function $\phi(q, t)$, which is known as distribution density function, level of interestingness, or strategic importance, indicates the specific weight of the point $q$ in that environment at time $t$. In this paper, the cost we are interested in is the quality of images when covering a spreading fire with a limited number of cameras. This notion of cost was first described in [10]. Since each camera has limited number of pixels to capture an image, it will provide one snapshot of the wildfire with lower resolution when covering it in a bigger FOV, and vice versa. By minimizing the information captured by the pixels of all the cameras, in other word, the area of the FOVs containing the fire, we could provide with optimal-resolution images of the fire. To quantify the cost, we first consider the image captured by one camera. From the relationship between object and image distance through a converging lens in classic optics, we can easily calculate the FOV area that a UAV covers (see Figure 2) as follows:

$$f(q, p_i) = \frac{S_1}{b^2}(b - z_i)^2, \forall q \in B_i, \tag{8}$$

where $q^T = [q_x, q_y]^T$ is the coordination of a given point that belongs to $Q(t)$, $S_1$ is the area of one pixel of a camera, and $b$ denotes the focal length. Note that, for a point $q$ to lie on or inside the FOV of a UAV $i$, it must satisfy the following condition:

$$\frac{||q - c_i||}{z_i} \leq \tan\theta. \tag{9}$$

From equation (8), it is obvious that the higher the altitude of the camera ($z_i$) is, the higher the cost the camera incures, or the lower its image resolution is.

For multiple cameras covering a point $q$, Schwager et al. [10] formulated a cost to represent the coverage of a point $q$ in a static field $Q$ over total number of pixels from a multiple of $n$ cameras as follows:

$$f_{N_q}(q, p_1, ..., p_n) = (\sum_{i \in N_q} f(p_i, q)^{-1})^{-1}, \tag{10}$$

where $f(p_i, q)$ calculated as in equation (8), $N_q$ is the set of UAVs that include the point $q$ in their FOVs. However, in case the point $q$ is not covered by any UAV, $f(p_i, q) = \infty$, the denominator in (10) can become zero. To avoid zero division, we need to introduce a constant $m$:

$$f_{N_q}(q, p_1, ..., p_n) = (\sum_{i \in N_q} f(p_i, q)^{-1} + m)^{-1}. \tag{11}$$

The value of $m$ should be very small, so that in such case, the cost in (11) become very large, thus discourage this case to happen. We further adapt the objective function (7) so that the UAVs will try to cover the field in the way that considers the region around the border of the fire more important. First, we consider that each fire front radiates a heat aura, as described in equation (4), Section II. The border region of each fire front has the least heat energy, while the center of the fire front has the most intense level. We assume that the UAVs equipped with infrared camera allowing them to sense different color spectra with respect to the levels of fire heat intensity. Furthermore, the UAVs are assumed to have installed an on-board fire detection program to quantify the differences in color into varying levels of fire heat intensity [4]. Let $I(q)$ denote the varying levels of fire heat intensity at point $q$, and suppose that the cameras have the same detection range $[I_{min}, I_{max}]$. The desired objective function that weights the fire border region higher than at the center of the fire allows us to characterize the importance function as follows:

$$\phi(q) = \kappa(I_{max} - I(q)) \quad = \kappa\Delta I(q). \tag{12}$$

One may notice that the intensity $I(q)$ actually changes over time. This makes $\phi(q)$ depends on the time, and would complicate equation (7) [16]. In this paper, we assume that the speed of the fire spreading is much less than the speed of the UAVs, therefore at a certain period of time, the intensity at a point can be considered constant. Also, note that some regions at the center of the wildfire may have $I = I_{max}$ now become not important. This makes sense because these regions likely burn out quickly, and they are not the goals for the UAV to track. We have the following objective function for wildfire coverage and tracking objective:

$$\min H = \int_{Q(t)} (\sum_{i \in N_q} f(p_i, q)^{-1} + m)^{-1} \kappa \Delta I(q) dq. \quad (13)$$

## IV. Controller Design

Figure 3 shows our controller architecture for each UAV. Our controller consists of two components: the coverage and tracking component and the potential field component. The coverage and tracking component calculates the position of the UAV for wildfire coverage and tracking. The potential field component controls the UAV to move to desired positions, and to avoid collision with other UAVs, as well as maintain the safety distance to the ground, by using potential field method. Upon reaching the wildfire region, the coverage and tracking control component will update the desired position of the UAV to the potential field control component. Assume the UAVs are quadcopters, then the dynamics of each UAV is:

$$u_i = \dot{p}_i, \quad (14)$$

we can then develop the control equation for each component in the upcoming subsections.

### A. Coverage & tracking control

Based on the artificial potential field approach [10], [19], [20], each UAV is controlled by a negative gradient (gradient descent) of the objective function $H$ in equation (13) with respect to its pose $p_i = [c_i, z_i]^T$ as follows:

$$u_i^{ct} = -k_s \frac{\partial H}{\partial p_i}, \quad (15)$$

where $k_s$ is the proportional gain parameter. The lateral position and altitude of each UAV is controlled by taking the partial derivatives of the objective function $H$ as follows:

$$\begin{aligned} \frac{\partial H}{\partial c_i} &= \sum_{k=1}^{4} \int_{Q(t) \cap l_{k,i}} (f_{N_q} - f_{N_q \setminus i}) n_k \kappa \Delta I dq, \\ \frac{\partial H}{\partial z_i} &= \sum_{k=1}^{4} \int_{Q(t) \cap l_{k,i}} (f_{N_q} - f_{N_q \setminus i}) \tan \theta^T n_k \kappa \Delta I dq, \\ &\quad - \int_{Q(t) \cap B_i} \frac{2 f_{N_q}^2}{\frac{S_1}{b^2} (b - z_i)^3} \kappa \Delta I dq, \end{aligned} \quad (16)$$

where $f_{N_q}$ and $f_{N_{q \setminus i}}$ are calculated as in equation (11), $N_q \setminus i$ denotes the coverage neighbor set excludes the UAV $i$, $n_k, k = 1:4$ denotes the outward-facing normal vectors of each edge, where $n_1 = [1, 0]^T$, $n_2 = [0, 1]^T$, $n_3 = [-1, 0]^T$, $n_4 = [0, -1]^T$. This set of equation is similar to the one proposed in [10], except that the environment $Q(t)$ now changes over the time, and the weight function $\phi(q)$ is characterized specifically for this problem. In (16), the component $\frac{\partial H}{\partial c_i}$ allows the UAV to move along $x$-axis and $y$-axis of the wildfire area which has $\Delta I$ is larger, while reduce the coverage intersections with other UAVs. The component $\frac{\partial H}{\partial z_i}$ allows the UAV to change its altitude along the $z$-axis to trade off between cover larger FOV (the first component) over the wildfire and to have a better resolution of the fire fronts propagation (the second component). From (16), the desired virtual position $p_{d_i}$ will be updated to the potential field control component (see Figure 3):

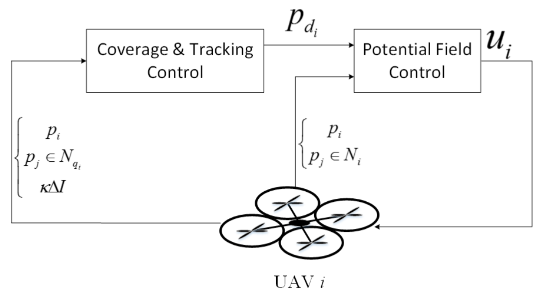


Fig. 3. Controller architecture of UAV $i$.

$$p_{d_i}(t + \Delta t) = p_{d_i}(t) - u_i^{ct} \Delta t, u_i^{ct} = (k_c \frac{\partial H}{\partial c_i}, k_z \frac{\partial H}{\partial z_i}). \quad (17)$$

### B. Potential field control

The objective of this component is to control a UAV from the current position to a new position updated from the coverage and tracking control. Similarly, our approach is to create an artificial potential field to induce each UAV to move to a desired position [21], [22] while avoiding in-flight collisions with other UAVs. We first create an attractive force to pull the UAVs to the initial rendezvous point $p_r$ by using a quadratic function of distance as the potential field, and take the gradient of it to yield the attractive force:

$$\begin{aligned} U_r^{att} &= \frac{1}{2} k_r ||p_r - p_i||^2 \\ u_i^r &= -\nabla U_r^{att} = -k_r(p_i - p_r). \end{aligned} \quad (18)$$

Similarly, the UAV moves to desired virtual position, $p_{d_i}$, passed from equation (17) in coverage & tracking component, by using this attractive force:

$$\begin{aligned} U_d^{att} &= \frac{1}{2} k_d ||p_{d_i} - p_i||^2 \\ u_i^d &= -\nabla U_d^{att} = -k_d(p_i - p_{d_i}). \end{aligned} \quad (19)$$

In order to avoid collision with its neighboring UAVs, we create repulsive forces from neighbors to push a UAV away if their distances become less than a designed safe distance $d$. Define the potential field for each neighbor UAV $j$ as:

$$U_j^{rep} = \begin{cases} \frac{1}{2} \nu (\frac{1}{||p_j - p_i||} - \frac{1}{d})^2, & if \ ||p_j - p_i|| < d \\ 0, & otherwise, \end{cases} \quad (20)$$

where $\nu$ is a constant. The repulsive force can be attained by taking the gradient of the sum of the potential fields created by all neighbor UAVs as follows:

$$
\begin{aligned}
u_i^{rep1} &= -\sum_{j\in N_i} a_{ij}\nabla U_j^{rep}\\
&= -\sum_{j\in N_i} \nu a_{ij}\Big(\frac{1}{||p_j-p_i||}-\frac{1}{d}\Big)\frac{1}{||p_j-p_i||^3}(p_i-p_j)\\
a_{ij} &= \begin{cases} 1, & if\ ||p_j-p_i||<d\\ 0, & otherwise.\end{cases}
\end{aligned}
\tag{21}
$$

Similarly, for maintaining a safe distance to the ground, we have:

$$
\begin{aligned}
u_i^{rep2} &= -a_{ii'}\nabla U_{i'}^{rep}\\
&= -\nu' a_{ii'}\Big(\frac{1}{||p_{i'}-p_i||}-\frac{1}{z_{min}}\Big)\frac{1}{||p_{i'}-p_i||^3}(p_i-p_{i'})\\
a_{ii'} &= \begin{cases} 1, & if\ ||p_{i'}-p_i||<z_{min}\\ 0, & otherwise.\end{cases}
\end{aligned}
\tag{22}
$$

From (18), (19), (21), and (22), we have the general control law for the potential field control component:

$$
\begin{aligned}
u_i = &-\sum_{j\in N_i} \nu a_{ij}\Big(\frac{1}{||p_j-p_i||}-\frac{1}{d}\Big)\frac{1}{||p_j-p_i||^3}(p_i-p_j)\\
&-\nu' a_{ii'}\Big(\frac{1}{||p_{i'}-p_i||}-\frac{1}{z_{min}}\Big)\frac{1}{||p_{i'}-p_i||^3}(p_i-p_{i'})\\
&-(1-\zeta_i)k_r(p_i-p_r)-\zeta_i k_d(p_i-p_{d_i}),\\
\zeta_i = &\begin{cases} 1, & if\ Q(t)\cap(B_i\cup l_{k,i})\neq\varnothing\\ 0, & if\ otherwise.\end{cases}
\end{aligned}
\tag{23}
$$

Note that, during the time the UAVs travel to the wildfire region, the coverage control component would not work because the sets $Q(t)\cap B_i$ and $Q(t)\cap l_{k,i}$ are initially empty, so $\zeta_i = 0$. Upon reaching the waypoint region where the UAVs can sense the fire, $\zeta_i = 1$, that would cancel the potential forces that draw the UAVs to the rendezvous point and let the UAVs track the fire fronts growing. The final position of the UAV $i$ will be updated as follows:

$$
p_i(t+\Delta t) = p_i(t) + u_i\Delta t. \tag{24}
$$

## V. SIMULATION

Our simulation was conducted in a Matlab environment. We started with 10 UAVs on the ground ($z_i = 0$) from a fire fighting center with initial location arbitrarily generated around $[300, 300]^T$. The safe distance was $d = 10$, and the safe altitude was $z_{min} = 15$. The UAVs were equipped with identical cameras with focal length $b = 10$, area of one pixel $S_1 = 10^{-4}$, half-angles $\theta_1 = 30°$, $\theta_1 = 45°$. We chose parameter $m = 1.5^{-5}$ to avoid zero division as in (11). The intensity sensitivity range of each camera was $[5, 100]^T$, and $\kappa = 10^{-3}$. The wildfire started with five initial fire front points near $[500, 500]^T$. The regulated mid-flame wind speed magnitude followed a Gaussian distribution with $\mu = 5mph$ and $\sigma = 2$. The wind flowed north-east direction with azimuth angle $\Theta$ also followed a Gaussian distribution with $\mu = \frac{\pi}{8}$ and $\sigma = 1$. The UAVs had a communication range $r = 500$. The coverage and tracking controller parameters were $k_c = 10^{-9}$, $k_z = 2^{-10}$, while the potential field controller parameters were $k_r = k_d = 0.06$, $\nu = 2.1$ and $\nu\prime = 10^3$. The simulation parameters were selected after numerous experiments.

We ran simulations in Matlab for 6000 time steps which yielded the result as shown in Figures 4 and 5. The wildfire spread continuously: the green areas depict the boundary with forest field and red areas represent the fire. The brighter red color area illustrates the fire front and regions near the boundary where the intensity was lower. The darker red colors show the area in fire with higher intensity. The UAVs came from the ground at $t = 0$ (Figure 5), and drove toward the wildfire region. The initial rendezvous point was $p_r = [500, 500, 60]^T$. Upon reaching the region near the initial rendezvous point at $[500, 500]^T$, the UAVs spread out to cover the entire wildfire (Figure 4-a). As the wildfire expanded, the UAVs fragment and follow the fire border regions (Figure 4-b, c, d). Note that the UAVs may not cover some regions with intensity $I = I_{max}$ (represented by black-shade color). Some UAVs may have low altitude if they cover region with small intensity $I$ (for example, UAV 5 in this simulation). The UAVs change altitude from $z_i \approx 60$ (Figure 5-a) to different altitudes (Figure 5-b, c, d), hence the area of the FOV of each UAV is different. The UAVs attempted to follow the fire front propagation, hence satisfying the tracking objective. Figure 6 shows the trajectory of each UAV in 3-dimensions while tracking the wildfire spreading north-east, and their current FOV on the ground.

## VI. CONCLUSION

In this paper, we presented a distributed control design for a team of UAVs that can collaboratively track a dynamic environment in the case of wildfire spreading. The UAVs can follow the border region of the wildfire as it keeps expanding, while still trying to maintain coverage of the whole wildfire. The UAVs are also capable of avoiding collision, maintaining safe distance to fire level, and are flexible in deployment. The application could certainly go beyond the scope of wildfire tracking, as the system can work with any dynamic environment, for instance, oil spilling or water flooding. In the future, more work should be considered to research about the hardware implementation of the proposed controller. For example, we should pay attention to the communication between the UAVs under the condition of constantly changing topology of the networks, or the sensing endurance problem in hazardous environment. Also, we would like to investigate the relation between the speed of the UAVs and the spreading rate of the wildfire, and attempt to synchronize it. Multi-drone cooperative sensing [23], [24] and cooperative learning [25] for wildland fire mapping will be also considered.

## REFERENCES

[1] "National interagency fire center." [Online]. Available: https://www.nifc.gov/fireInfo/fireInfo_statistics.html

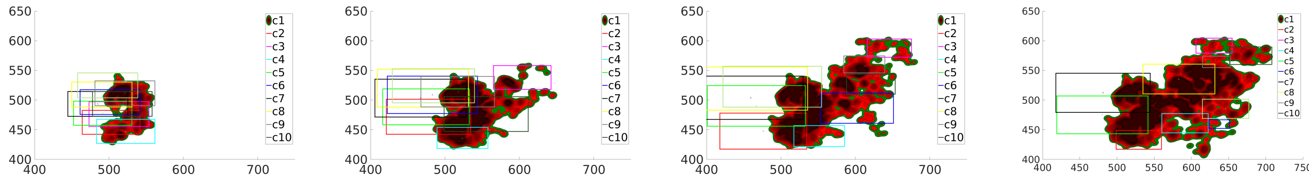


(a) t = 1000 (b) t = 3000 (c) t= 4000 (d) t = 6000

Fig. 4. Simulation result shows the field of view of each UAV on the ground in a) t = 1000, b) t = 3000, c) t= 4000, and d) t = 6000.

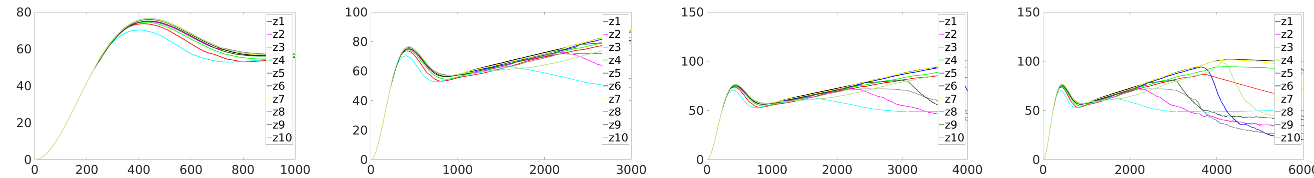


(a) t = 1000 (b) t = 3000 (c) t= 4000 (d) t = 6000

Fig. 5. Plot shows the altitude of each UAV on the ground in a) t = 1000, b) t = 3000, c) t= 4000, and d) t = 6000.

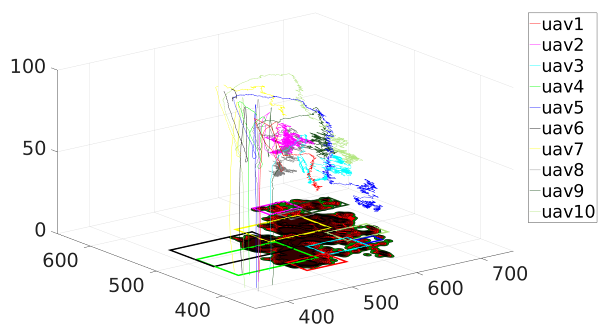


Fig. 6. 3D representation of the UAVs tracking the fire.

[2] J. R. Martinez-de Dios, B. C. Arrue, A. Ollero, L. Merino, and F. Gómez-Rodríguez, "Computer vision techniques for forest fire perception," *Image and vision computing*, vol. 26, no. 4, pp. 550–562, 2008.

[3] L. Merino, F. Caballero, J. Martnez-de Dios, J. Ferruz, and A. Ollero, "A cooperative perception system for multiple uavs: Application to automatic detection of forest fires," *Journal of Field Robotics*, vol. 23, no. 3-4, pp. 165–184, 2006.

[4] H. Cruz, M. Eckert, J. Meneses, and J.-F. Martínez, "Efficient forest fire detection index for application in unmanned aerial systems (uass)," *Sensors*, vol. 16, no. 6, p. 893, 2016.

[5] C. Yuan, Z. Liu, and Y. Zhang, "Uav-based forest fire detection and tracking using image processing techniques," in *Unmanned Aircraft Systems (ICUAS), 2015 International Conference on*, June 2015, pp. 639–643.

[6] D. Casbeer, R. Beard, T. McLain, S.-M. Li, and R. Mehra, "Forest fire monitoring with multiple small uavs," in *American Control Conference, 2005. Proceedings of the 2005*, June 2005, pp. 3530–3535 vol. 5.

[7] M. Kumar, K. Cohen, and B. HomChaudhuri, "Cooperative control of multiple uninhabited aerial vehicles for monitoring and fighting wildfires," *Journal of Aerospace Computing, Information, and Communication*, vol. 8, no. 1, pp. 1–16, 2011.

[8] C. Phan and H. H. Liu, "A cooperative uav/ugv platform for wildfire detection and fighting," in *System Simulation and Scientific Computing, 2008. ICSC 2008. Asia Simulation Conference-7th International Conference on*. IEEE, 2008, pp. 494–498.

[9] C. Yuan, Y. Zhang, and Z. Liu, "A survey on technologies for automatic forest fire monitoring, detection, and fighting using unmanned aerial vehicles and remote sensing techniques," *Canadian journal of forest research*, vol. 45, no. 7, pp. 783–792, 2015.

[10] M. Schwager, B. J. Julian, M. Angermann, and D. Rus, "Eyes in the sky: Decentralized control for the deployment of robotic camera networks," *Proceedings of the IEEE*, vol. 99, no. 9, pp. 1541–1561, 2011.

[11] R. C. Rothermel, "A mathematical model for predicting fire spread in wildland fuels," 1972.

[12] G. D. Richards, "An elliptical growth model of forest fire fronts and its numerical solution," *International Journal for Numerical Methods in Engineering*, vol. 30, no. 6, pp. 1163–1179, 1990.

[13] M. A. Finney *et al.*, *FARSITE: Fire area simulator: model development and evaluation*. US Department of Agriculture, Forest Service, Rocky Mountain Research Station Ogden, UT, 2004.

[14] T. M. Williams, B. J. Williams, and B. Song, "Modeling a historic forest fire using gis and farsite," *Mathematical & Computational Forestry & Natural Resource Sciences*, vol. 6, no. 2, 2014.

[15] J. Cortes, S. Martinez, T. Karatas, and F. Bullo, "Coverage control for mobile sensing networks," *IEEE Transactions on robotics and Automation*, vol. 20, no. 2, pp. 243–255, 2004.

[16] L. C. Pimenta, M. Schwager, Q. Lindsey, V. Kumar, D. Rus, R. C. Mesquita, and G. A. Pereira, "Simultaneous coverage and tracking (scat) of moving targets with robot networks," in *Algorithmic foundation of robotics VIII*. Springer, 2009, pp. 85–99.

[17] M. Schwager, D. Rus, and J.-J. Slotine, "Decentralized, adaptive coverage control for networked robots," *The International Journal of Robotics Research*, vol. 28, no. 3, pp. 357–375, 2009.

[18] A. Breitenmoser, M. Schwager, J.-C. Metzger, R. Siegwart, and D. Rus, "Voronoi coverage of non-convex environments with a group of networked robots," in *Robotics and Automation (ICRA), 2010 IEEE International Conference on*. IEEE, 2010, pp. 4982–4989.

[19] A. C. Woods and H. M. La, "A novel potential field controller for use on aerial robots," *IEEE Transactions on Systems, Man, and Cybernetics: Systems*, 2017.

[20] H. M. La and W. Sheng, "Dynamic target tracking and observing in a mobile sensor network," *Robotics and Autonomous Systems*, vol. 60, no. 7, pp. 996 – 1009, 2012. [Online]. Available: http://www.sciencedirect.com/science/article/pii/S0921889012000565

[21] A. C. Woods, H. M. Lay, and Q. P. Ha, "A novel extended potential field controller for use on aerial robots," in *2016 IEEE International Conference on Automation Science and Engineering (CASE)*, Aug 2016, pp. 286–291.

[22] A. C. Woods and H. M. La, *Dynamic Target Tracking and Obstacle Avoidance using a Drone*. Cham: Springer International Publishing, 2015, pp. 857–866. [Online]. Available: https://doi.org/10.1007/978-3-319-27857-5_76

[23] H. M. La and W. Sheng, "Distributed sensor fusion for scalar field mapping using mobile sensor networks," *IEEE Transactions on Cybernetics*, vol. 43, no. 2, pp. 766–778, April 2013.

[24] H. M. La, W. Sheng, and J. Chen, "Cooperative and active sensing in mobile sensor networks for scalar field mapping," *IEEE Transactions on Systems, Man, and Cybernetics: Systems*, vol. 45, no. 1, pp. 1–12, Jan 2015.

[25] H. M. La, R. Lim, and W. Sheng, "Multirobot cooperative learning for predator avoidance," *IEEE Transactions on Control Systems Technology*, vol. 23, no. 1, pp. 52–63, Jan 2015.